

## Determination of the neutron resonance parameters for $^{209}\text{Bi}$ from new capture and transmission measurements at GELINA

A. Borella<sup>\*1</sup>, F. Gunsing<sup>1</sup>, S. Kopecky<sup>2</sup>, P. Mutti<sup>3</sup>, P. Schillebeeckx<sup>2</sup>,  
P. Siegler<sup>2</sup> and R. Wynants<sup>2</sup>

<sup>1</sup>CEA DAPNIA/SPhN F-91911 Gif-sur-Yvette Cedex, France

<sup>2</sup>EC-JRC-IRMM, Retieseweg 111, B-2440 Geel, Belgium

<sup>3</sup>Institut Laue-Langevin, rue Jules Horowitz 6, F-38042 Grenoble, France

### Abstract

High resolution neutron total and capture cross section measurements have been performed to determine the resonance parameters for  $^{209}\text{Bi} + n$ . The transmission and capture measurements were carried out at the time-of-flight facility GELINA of the IRMM in Geel (Belgium).

The transmission measurements were carried out at a 30 m and a 50 m flight path using Li-glass scintillators. The capture measurements were performed at a 30 m and 60 m flight path based on the total energy detection principle. The capture detection system consisted of four  $\text{C}_6\text{D}_6$  detectors and a  $^{10}\text{B}$  ionization chamber, which was used to determine the shape of the neutron flux.

A special analysis procedure, including a sample dependent pulse height weighting function, was applied to ensure that the efficiency for a neutron capture event was independent from the  $\gamma$ -ray cascade. From a simultaneous resonance shape analysis of the transmission and capture data we deduced the neutron width for 10 resonances and the capture area for 43 resonances up to a neutron energy of 40 keV. The resonance shape analysis was performed with the most recent version of the REFIT code. This latest version includes a direct correction for the neutron sensitivity of the capture detection system and accounts for the influence of the neutron attenuation in the sample on the weighted response.

**KEYWORDS:** *TOF-measurements, total and capture cross section, resonance parameters, bismuth, ADS*

## 1. Introduction

The most promising Accelerator Driven System (ADS) development proposes the use of lead-bismuth eutectic as spallation target, coolant and moderator. Since the neutron induced total and capture cross sections of  $^{209}\text{Bi}$  are important for the safe operation of an ADS and for long-term disposal aspects, an accurate knowledge of the neutron resonance parameters for  $^{209}\text{Bi}$  is required. Moreover, accurate neutron capture cross section data are important in astrophysics for the understanding of the end point of the s-process path.

The experimental neutron cross section data for Pb-isotopes and  $^{209}\text{Bi}$  are rather scarce. In the resolved resonance region, the experiments were primarily performed in support to fundamental

---

\* Corresponding author; Tel. +33 1 6908 7451, Fax. +33 1 6908 7584, E-mail: [alessandroborella@yahoo.it](mailto:alessandroborella@yahoo.it)

physics research, such as doorway states in closed shell regions, and to astrophysics applications. For  $^{209}\text{Bi}$  previously two sets of transmission data [1,2] and three sets of capture data are available [3,4,5]. These capture data may suffer from a systematic bias effect up to 6 % since the total  $\gamma$ -ray energy released in the capture reaction, necessary for the pulse height weighting technique, is generally unknown because of the isomeric state in  $^{210}\text{Bi}$  at 271 keV. An average value of the branching has been applied previously since this quantity as a function of neutron energy is not well known. The determination of the energy dependent ratio of the population of the ground state and of the isomeric state following neutron capture is discussed in a separate contribution to this conference [6].

To improve the cross section data for  $^{209}\text{Bi}$  a series of total and capture cross section measurements were recently performed at the GELINA facility of the IRMM. We improved the data reduction by accounting for capture to the isomeric state and the influence of the sample properties on the effective response. In this paper the results of a preliminary data analysis are reported. The analysis did not include the data of Mutti et al. [4].

Transmission and capture measurements were carried out at the neutron time-of-flight (TOF) spectrometer GELINA. The accelerator was operated at 800 Hz and 70  $\mu\text{A}$  average electron current, providing electron pulses of 1 ns with 100 MeV average electron energy. A detailed description of GELINA can be found in Ref. [7].

## 2. Transmission Measurements

The transmission measurements were performed at two different flight paths using lithium glass scintillators as neutron detectors. The Li-glass was mounted in an Al canning and viewed by two EMI 9823 KQB photomultipliers, which were placed outside the neutron beam. Two  $\text{BF}_3$  proportional counters were used to monitor the neutron flux of the accelerator and to normalize the spectra. Air conditioning was installed at the measurement and sample station to keep the sample at a constant temperature and to reduce electronic drifts due to temperature changes. The temperature at the sample position was continuously monitored. The average temperature was then used in the analysis program to calculate the Doppler broadening of the resonances.

Measurements at a 26 m flight path were carried out to deduce the neutron widths of the strong *s*-wave resonances at 800 eV and 2319 eV. The measurements were performed on a 0.3 mm thick sample of metallic bismuth, corresponding to a thickness of  $8.84 \times 10^{-4}$  at/b. The angle between the electron beam and the flight path was  $99^\circ$ . At 9.1 m distance from the neutron producing target the bismuth sample was placed in an automatic sample changer, operated by the data acquisition system. The sample changer was placed behind a 294 mm long collimator with an aperture that results in a 15 mm diameter beam at the sample. A 0.0129 at/b thick  $^{10}\text{B}$  anti-overlap filter was placed just before the sample changer. Measurements with “black” resonance filters (S, Na, Bi and Co) were carried out in order to deduce the background. After the filters and the sample, the neutron beam was further collimated and finally detected by a Li-glass scintillator (NE 912), placed at 26.5 m from the neutron producing target. The Li-glass had a 110 mm effective diameter and 12.7 mm thickness. The dead time of the detector system was 1160 (8) ns.

For the weaker *s*-wave resonances up to 40 keV measurements were performed at a 49.6 m flight path. The measurements were carried out on a 4 mm thick sample of metallic bismuth corresponding to a thickness of  $1.08 \times 10^{-2}$  at/b. The angle between the electron beam and the

flight path was  $81^\circ$ . At approximately 25 m distance from the neutron producing target the bismuth sample was placed in an automatic sample changer, operated by the data acquisition system. The sample changer was placed behind a 400 mm long collimator with an aperture that results in an approximately 45 mm diameter beam at the sample. The 0.04 at/b thick  $^{10}\text{B}$  anti-overlap filter together with a thick sample of lead was placed at approximately 10 m from the neutron producing target. The background was estimated using the black resonances of S and Na. The procedure for correcting the background was checked using thick samples of Ge and Cu. After the filters and the sample, the neutron beam was further collimated and finally detected by a Li-glass scintillator (NE 912), placed at 49.6 m from the neutron producing target. The Li-glass had a 101.6 mm effective diameter and 6.35 mm thickness. The dead time of the detector system was 2050 (10) ns.

### 3 Capture Measurements

In order to verify the capture area of the resonances up to 40 keV neutron energy, new capture measurements were performed at a 28.7 and 58.6 m flight path station. The  $\gamma$ -rays, originating from the capture reaction in the sample, were detected in four  $\text{C}_6\text{D}_6$ -based liquid scintillators (NE230) of 10 cm diameter and 7.5 cm height. Each scintillator was coupled to an EMI 9823 KQB photomultiplier through a quartz window.

For the measurements at 30 m, the angle between the electron beam and the flight path was  $-90^\circ$ . The moderated neutron beam was collimated to about 25 mm in diameter at the sample position. To reduce the contribution of overlap neutrons we used a 0.018 at/b thick  $^{10}\text{B}$  anti-overlap filter. The “black” resonance in sulphur at 102.7 keV was used to monitor the amplitude of the background. The bismuth sample consisted of a metallic bismuth disc of 19.95 mm diameter and 1.0 mm thickness ( $2.76 \times 10^{-3}$  at/b). Such a thickness allowed the determination of the capture area of the strongest s-waves resonances up to 40 keV neutron energy, reducing the effect of the multiple scattering. The shape of the neutron spectrum was measured with a Frisch-gridded ionization chamber placed 60 cm before the sample. This chamber was loaded with one back-to-back layers of about  $40 \mu\text{g}/\text{cm}^2$   $^{10}\text{B}$ .

To determine the capture area of the weaker resonances up to 40 keV neutron energy, additional capture measurements were performed at a 60 m flight path station. The angle between the flight path and the normal of the moderator for this flight path was  $-81^\circ$ . The moderated neutron beam was collimated to about 75 mm in diameter at the sample position. To reduce the contribution of overlap neutrons we used a 0.0416 at/b thick  $^{10}\text{B}$  anti-overlap filter. The “black” resonance in sulphur at 102.7 keV was used to monitor the amplitude of the background. The bismuth sample consisted of a metallic bismuth disc of 80 mm diameter and 3.0 mm thickness ( $8.34 \times 10^{-3}$  at/b). The shape of the neutron spectrum was measured with a triple Frisch-gridded ionization chamber placed 80 cm before the sample. This chamber was loaded with three back-to-back layers of about  $40 \mu\text{g}/\text{cm}^2$   $^{10}\text{B}$  each.

To determine the capture cross section the total energy detection principle in combination with the Pulse Height Weighting Technique (PHWT) [8] is applied. We used Monte Carlo simulations to deduce a weighting function which accounts for the influence of the sample characteristics on the final response of the capture detection system [9]. In this calculation it is assumed that the  $\gamma$ -rays are produced uniformly across the sample as the attenuation of the incident neutron flux is small. To account for the effective distribution of  $\gamma$ -rays in the sample, a correction factor was deduced for the 3 mm sample. This factor is dependent on the total cross

section and its determination is based on Monte Carlo simulations described in [9]. Since the total cross section is not known a priori, the resonance shape analysis code REFIT was modified to account for this correction.

The normalization of the bismuth data was determined from measurements on  $^{nat}\text{Fe}$ , using the 1.15 keV resonance of  $^{56}\text{Fe}$ . The resonance shape analysis was performed in the region around the 1.15 keV resonance, fitting only the normalization and background level and assuming a neutron width of 61.7 meV and a radiation width of 574 meV.

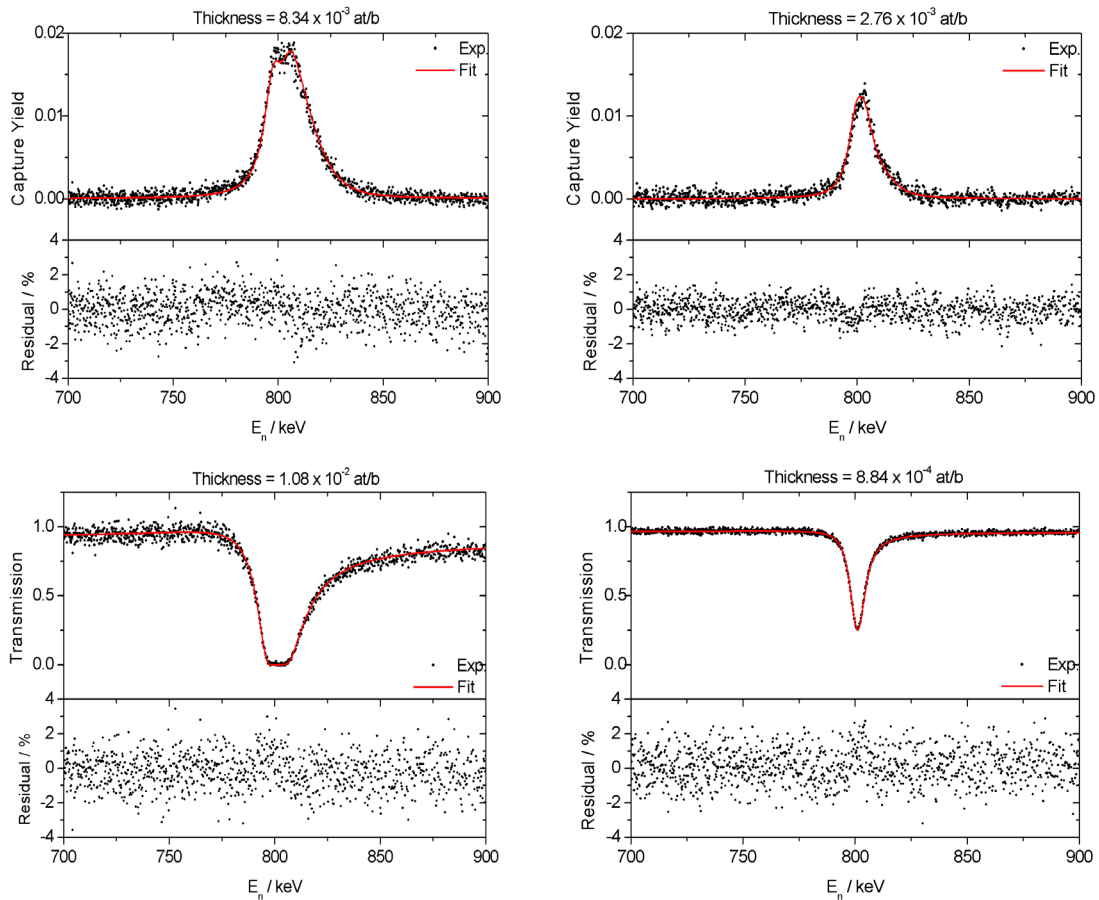
## 4 Results and Discussion

To derive the transmission factors and capture yields from the raw TOF spectra we used the data processing package AGS (Analysis of Generalized Spectra) developed at the IRMM. This package allows full covariance propagation in the data reduction and will also be presented at this conference [10]. The capture data were reduced assuming 50 % branching in the population of the metastable state at 271 keV. This resulted in an increase of the yield by 3.3 %, compared to the case where no population of the metastable state is considered. Moreover, the data were corrected to account for the experimental threshold at 150 keV and for the internal conversion on the two intense low-energy transitions of 160 keV and 310 keV  $\gamma$ -ray energy. This resulted in an increase of the yield by 2.74 %.

The Resonance Shape Analysis (RSA) is performed with the latest version of REFIT [11]. This version includes a direct correction for the neutron sensitivity of the capture detection system and accounts for the influence of the neutron attenuation in the sample on the weighted response. We verified that the impact of this correction on the 800 eV resonance results in a reduction of the capture area by 11 %.

The background of the capture data is given by the sum of two time dependent components and this correction is included in the REFIT code. The first time dependent component, the non-prompt background contribution, can be estimated from the capture yield between well-separated resonances and depends strongly on the measurement conditions and collimators installed at neighboring flight paths. The second component, the so-called prompt background, originates from neutrons, which are scattered in the sample and subsequently captured in the detector environment. This contribution is hard to distinguish from a capture event in the sample and it contributes directly to the resonance area and is related to the neutron sensitivity of the detector. The contribution of this component was estimated with Monte Carlo simulations as explained in [9]. This component is particularly important in nuclei with large scattering to capture ratio, as  $^{209}\text{Bi}$ . The impact of this background component calculated by carrying out a RSA with and without neutron sensitivity. When neglecting the prompt background the capture area resulted to be higher by 5 % and 14 % for the 12.1 keV and 15.5 keV s-wave resonances, which show the highest scattering to capture ratio.

**Figure 1:** The results of the simultaneous RSA of capture and transmission data for the s-wave resonance at 800 eV.



The resonance parameters and the scattering radius were deduced from the simultaneous RSA of two transmission factor and three capture yields. The starting values of the resonance parameters were the one given by ENDF/B-VI.8 adding the resonance quoted by Mutti [4]. For the analysis of the weaker resonances which could only be seen in capture, we proposed initially to use the neutron widths quoted by ENDF/B-VI.8. The data have been analyzed up to a neutron energy of 40 keV. The resulting fit of the data sets in the energy range for the s-wave resonance at 800 eV is shown in Fig. 1. This chi-squared per degree of freedom on the energy regions of interest was around unity.

The neutron widths for the 10 most intense s-waves were deduced. In Fig. 2 and 3 we plot the ratio between the neutron width deduced in this work and the one quoted in [1, 2]. Fig. 2 and 3 reveal that the neutron widths of [1, 2] are systematically lower than our results.

**Figure 2:** The ratio between the neutron widths obtained in this work and the ones given in Ref. [1] between 0 and 40 keV. The error bar resulted from the combination of the quoted uncertainty in Ref. [1] and the uncertainty on our results. The latter is a combination of the statistical uncertainty and a 5 % systematic uncertainty.

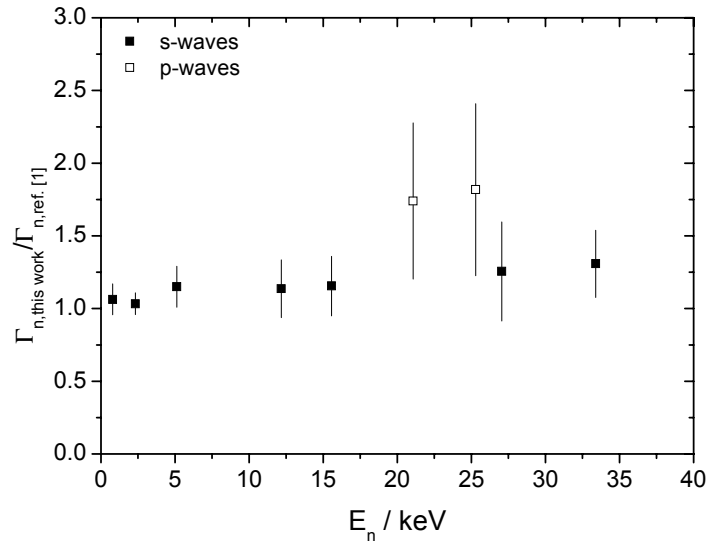
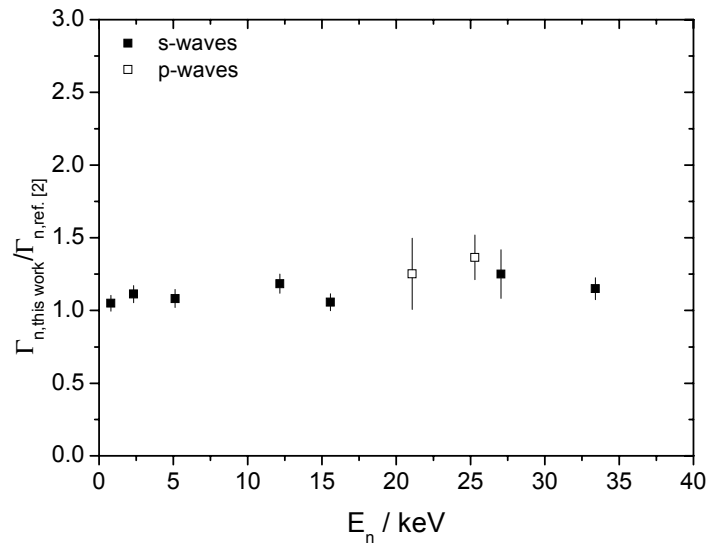


**Figure 3:** The ratio between the neutron widths obtained in this work and the ones given in Ref. [2] between 0 and 40 keV. The error bar resulted from the combination of the quoted uncertainty in Ref. [2] and the uncertainty on our results. The latter is a combination of the statistical uncertainty and a 5 % systematic uncertainty.



In Fig. 4, 5 and 6 we compare the capture area obtained in this work with the one quoted in Ref. [3], [4] and [5], respectively. Up to an energy of 40 keV we could observe 43 resonances. Mutti observed 44 resonance in the same energy interval. Macklin observed 42 resonances and the resonances at 9.4 keV, 23.85 keV, 24.2 keV and 27.45 keV quoted by Macklin et al. [3], were not seen in our capture data. This is confirmed by Mutti [4] and indicates a possible presence of impurities in the sample used by Macklin et al.. Due to the presence of a permanent S filter in the capture measurements, the resonance at 30.49 keV could not be observed. Domingo et al. [5] could observe only 19 resonances up to 23 keV, while we observed 24 resonances in the same energy interval. In particular they did not observe the strong s-wave at 15 keV.

**Figure 4:** The ratio between the capture area ( $A$ ) obtained in this work and the ones given in Ref. [3] between 0 and 40 keV. Only well-isolated resonances with a statistical uncertainty smaller than 10 % are shown. The error bar resulted from the combination of the quoted uncertainty in Ref. [3] and the uncertainty on our results. The latter is a combination of the statistical uncertainty and a 5 % systematic uncertainty.

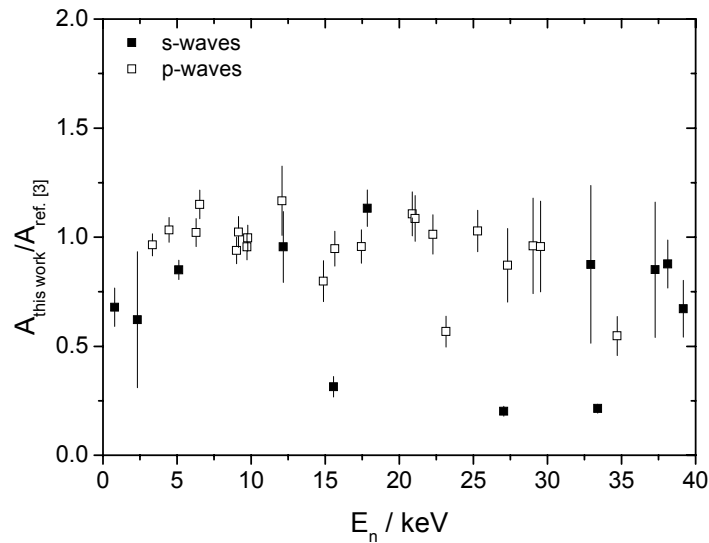


**Figure 5:** The ratio between the capture area ( $A$ ) obtained in this work and the ones given in Ref. [4] between 0 and 40 keV. Only well-isolated resonances with a statistical uncertainty smaller than 10 % are shown. The error bar resulted from the combination of the quoted uncertainty in Ref. [4] and the uncertainty on our results. The latter is a combination of the statistical uncertainty and a 5 % systematic uncertainty.

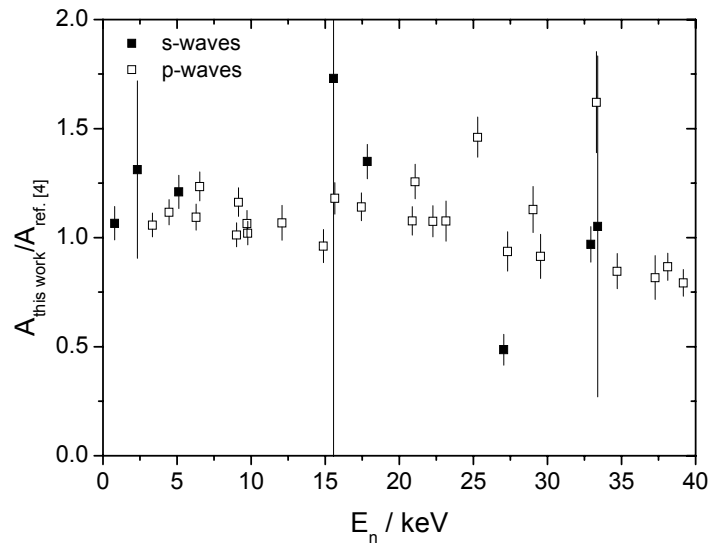
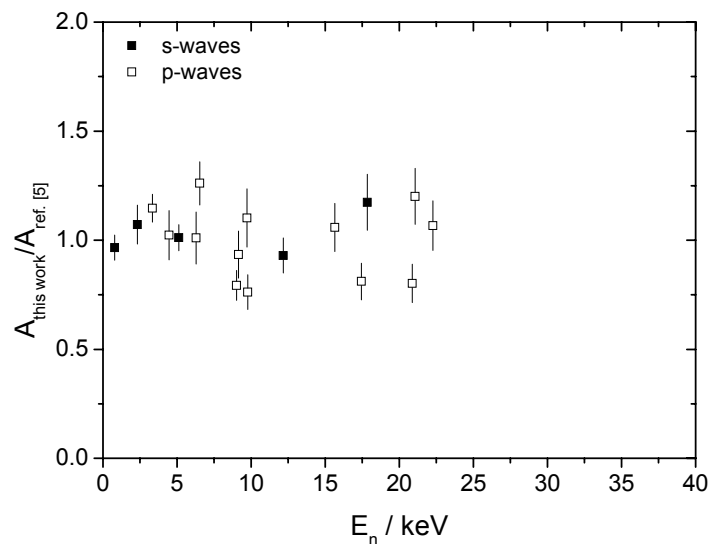


**Figure 6:** The ratio between the capture area ( $A$ ) obtained in this work and the ones given in Ref. [5] between 0 and 40 keV. Only well-isolated resonances with a statistical uncertainty smaller than 10 % are shown. The error bar resulted from the combination of the quoted uncertainty in Ref. [6] and the uncertainty on our results. The latter is a combination of the statistical uncertainty and a 5 % systematic uncertainty.





We observe a systematic deviation from Macklin's data for all the s-wave resonances except the one at 17.8 keV. This deviation may be ascribed to an overestimation of the neutron sensitivity correction.

When comparing our capture area with the one of Domingo et al., we do not observe a systematic deviation of the results. The data agree for most of the resonances within the error bar. The capture areas of Mutti are systematically lower than our results up to an energy of 25 keV. This deviation can be ascribed to the use of a weighting function not accounting for the photon transport in the sample in [9]. Moreover, for the s-wave resonance at 15.5 keV, Mutti quotes a capture area with 100% uncertainty due to the large correction for neutron sensitivity on this resonance. Above 25 keV the capture areas of Mutti and Macklin seems to be overestimated. Again, this might be due to an underestimation of the neutron component. As shown in [9], between 25 keV and 40 keV, the resonances of  $^{27}\text{Al}$  and  $^{19}\text{F}$  contribute to the neutron sensitivity of the detection system.

The observed difference on specific resonances may be due to several effects: poor resolution in time-of-flight, neutron sensitivity correction, different total energy due to the used branching ratio, uncertainty related to PHWT (weighting function calculation, effect of threshold and the coupling between photon and neutron transport).

## 5 Conclusions

We performed neutron total and capture cross section measurements on  $^{209}\text{Bi}$  at GELINA in an energy range up to 40 keV with a 1 ns time resolution. A comparison of our capture data with the data in the literature reveals discrepancies of up to 20 – 30 %. These discrepancies result from systematic uncertainties due to low energy resolution, uncertainty on the branching ratio, the neutron sensitivity of the detectors and the use of weighting function not accounting for the gamma transport in the sample and coupling between  $\gamma$ -ray and neutron transport due to neutron flux attenuation in the sample. The resonance parameters deduced from our transmission data are systematically higher than the data quoted in [1, 2].

To confirm this systematic effect, new transmission measurements on thicker samples are scheduled. A new data analysis including Mutti's data, which are the best available in terms of counting statistics and signal to background ratio, and including the results of the branching ratio experiments is foreseen.

## Acknowledgements

The authors would like to thank Wim Mondelaers and his staff for the skilful operation of the accelerator. We are also grateful to J. Gonzalez for his technical support.

## References

- 1) U.N. Singh, J. Rainwater, H.L. Liou, G. Hacken and J.B. Garg, "Neutron resonance spectroscopy :  $^{209}\text{Bi}$ ", Phys. Rev. C13, 124 (1976)
- 2) A. R. de L. Musgrove and J.A. Harvey, "Neutron resonance spectroscopy on  $^{209}\text{Bi}$ " Aust. J. Phys. 31, 47 (1978)
- 3) R. Macklin and J. Halperin, "Resonance neutron capture on  $^{209}\text{Bi}$ ", Phys. Rev. C14, 1389 (1976)
- 4) P. Mutti et al., PhD thesis, Gent University, 1997

- 5) C. Domingo et al., “New measurement of neutron capture resonances of  $^{209}\text{Bi}$ ” submitted to Phys. Rev. C
- 6) A. Borella et al., contribution to this conference
- 7) D. Tronc, J.M. Salomé, and K.H. Böckhoff, “A new pulse compression system for intense relativistic electron beams”, Nucl. Instr. Meth. 228, 217 (1985)
- 8) R.L. Macklin and J.H. Gibbons, “Capture-Cross-Section Studies for 30-220-keV Neutron Using a New Technique”, Phys. Rev, 159, 1007 (1967)
- 9) A. Borella, G. Aerts, F. Gunsing, P. Schillebeeckx, in preparation
- 10) P. Schillebeeckx et al., contribution to this conference
- 11) M.C. Moxon and J.B. Brislan, Technical Report Harwell Laboratory, CBNM/ST/90-131/1